Hindawi
Mathematical Problems in Engineering
Volume 2022, Article ID 5337569, 10 pages
https://doi.org/10.1155/2022/5337569

Research Article

Landweber Iteration-Inspired Network for Image Super-Resolution

Xiaohui Li,[1] **Ling Wang**,[2] **and Xinbo Liu**[3,4]

[1]*School of Electronics and Information Engineering, Liaoning University of Technology, Jinzhou, China*
[2]*School of Materials Science and Engineering, Yingkou Institute of Technology, Yingkou, China*
[3]*Key Laboratory of Security for Network and Data in Industrial Internet of Liaoning Province, Liaoning University of Technology, Jinzhou, China*
[4]*SolBridge International School of Business, Woosong University, Daejeon, Republic of Korea*

Correspondence should be addressed to Xinbo Liu; lxb715@hotmail.com

Received 20 April 2022; Revised 14 May 2022; Accepted 21 May 2022; Published 20 June 2022

Academic Editor: Nouman Ali

Copyright © 2022 Xiaohui Li et al. This is an open access article distributed under the Creative Commons Attribution License, which permits unrestricted use, distribution, and reproduction in any medium, provided the original work is properly cited.

Image super-resolution (SR) is one of the classical ill-posed image processing issues to generate high-resolution (HR) images from given low-resolution (LR) instances. Recent SR works aim to find an elaborate convolutional neural network (CNN) design and regard it as an end-to-end filter to map the image from LR space to HR space. However, seldom of them concentrate on the mathematical proof of network design or consider the problem from an optimization perspective. In this paper, we investigate the image SR based on the Landweber iteration method, which is an effective optimization method to find a feasible solution for the ill-posed problem. By considering the issue from the optimization perspective, we design a corresponding Landweber iteration-inspired network to adaptively learn the parameters and find the HR results. Experimental results show the proposed network achieves competitive or better subjective and objective performance than other state-of-the-art methods with fewer parameters and computational costs.

1. Introduction

Single image super-resolution (SISR), one of the classical image processing issues, has been widely investigated in recent years. Given a low-resolution (LR) image, the task of SISR is to generate a corresponding high-resolution (HR) instance with satisfying visual quality [1]. Image super-resolution (SR) has been widely investigated in numerous applications, such as image inpainting [2], self-driving [3], pose detection [4], underwater image enhancement [5], video deinterlacing [6], and recognition [7]. Figure 1 shows an example of image super-resolution. Figure 1(a) shows the given low-resolution image and the original high-resolution instance. Figure 1(b) shows the restored SR images.

Traditional SISR methods usually find a feasible solution for SISR by interpolation or compressed sensing. Zhang et al. proposed a contourlet-based interpolation method for SISR [8]. There are also works conducting the interpolation with the help of wavelet transformation [9]. Recently, rational fractal interpolation is also considered for image SR [10]. These works aim to design a filter to process the image but lack the learning step for finding the statistical correlation between LR and HR images. Compressed sensing for SISR, which learns a mapping relationship between LR and HR images from training data, is also fully investigated by researchers. Chen et al. utilized K-SVD for dictionary learning and achieved good restoration performance [11]. Zhao et al. considered local manifold projection in compressed sensing for more accurate results [12]. The compressed sensing-based methods highly depend on the choice of regulation term. Furthermore, the hyper-parameters are manually intervened and lack the ubiquity.

With the rapid development of deep learning, recently there are convolutional neural networks (CNNs) specially designed for SISR, which achieve state-of-the-art performance. SRCNN [13] is the first CNN-based method for SISR

(a) (b)

Figure 1: An example of image super-resolution. (a) The given low-resolution (LR) image and the original high-resolution (HR) instance. (b) The restored super-resolution (SR) image.

with a three-layer neural network to simulate the step of compressed sensing. After SRCNN, numerous works are devising elaborate blocks to build the CNN deeper and wider. VDSR [14] proposed a very deep network with residual connection for improving the performance. EDSR [15] removed the batch normalization and built the network with residual blocks [16]. In recent years, RDN [17], DRN [18], RFANet [19], and other works design effective blocks to achieve state-of-the-art performance. However, these works only concentrate on the network architecture, but almost neglect to consider the mathematical proof of the design.

There are also works considering the SISR from the optimization perspective. IRCNN [20] analyzed the image restoration by half-quadratic splitting (HQS) strategy and designed an end-to-end network for multitask image restoration. Hu et al. devised an end-to-end network inspired by the alternating direction method of multipliers (ADMM) [21]. Liu et al. also proposed a novel network termed ISRN [22] for restoration, which is inspired by the HQS strategy. However, these works only use stacked blocks to build the solver of iterative formulations, but do not concentrate on guiding the block design itself by the optimization method.

In this paper, we design a novel Landweber iteration [23] inspired network for SISR, which is termed as LandNet. Different from other iteration optimization-inspired CNN-based methods, the proposed LandNet unfolds the iteration steps into sequential network blocks, and designs a straightforward network to generate HR images from LR instance. Specially, we devise a novel block inspired by the formulation of Landweber iteration, and use convolutional layers to simulate the optimization step of each iteration. Based on the unfolding blocks, an end-to-end network is established for effective restoration. Experimental results show the proposed LandNet achieves competitive or better subjective and objective performance than other state-of-the-art methods with fewer parameters and computation cost.

The contribution of this paper can be concluded as

(i) We analyze the image super-resolution in the optimization perspective and design a novel block for restoration inspired by the Landweber iteration method.

(ii) We design an unfolding network for end-to-end image super-resolution based on the proposed optimization block, which is termed as LandNet.

(iii) Experiment results show that the proposed LandNet achieves competitive or better subjective and objective performance than other works with fewer parameters and computation cost.

2. Relate Works

Image processing and analysis is an important task for signal processing [24, 25]. As a classical issue in image processing, the task of image super-resolution (SR) is to generate high-resolution (HR) images from low-resolution (LR) instances [26–28]. In recent years, convolutional neural networks (CNNs) have demonstrated amazing performance on image SR. SRCNN [13] is the first CNN-based image super-resolution network that achieves a large improvement over traditional works. FSRCNN [29] improves the speed of SRCNN and utilizes a deeper network to obtain a better performance. ESPCN [30] proposes a subpixel convolution strategy to resize the feature map and utilizes it to substitute the deconvolutional layer, which has been widely used in recent works. VDSR [14], EDSR [15], and SRDenseNet [31] build the network deeper and wider for better performance. In recent years, more and more elaborate blocks are proposed for effective restoration. RDN [17] combines the residual [16] and dense [32] connections and designs a novel residual dense block for image restoration. RCAN [33] investigates a residual-in-residual block with channel-wise attention [34] and achieves the state-of-the-art performance. SAN [35] utilizes a second-order attention network to focus on the inherent correlations among features. RFANet [19] aggregates the residual information to improve the network representation. Based on the residual aggregation, RFDN [36] is also proposed for effective lightweight image super-resolution. These works build the network with well-designed blocks and achieve good performances. Cross-SRN [7] designs a cross convolution to enhance the edge information recovery. Zhu et al. devised a GAN-based method for perceptual-oriented image super-resolution [37]. Recently, there are effective networks specially designed for image and video super-resolution. Mei et al. combined the nonlocal attention and the sparse representation for image super-resolution and proposed a novel nonlocal sparse attention with dynamic sparse attention pattern for image super-resolution, which achieved the state-of-the-art performance [38]. Jiang et al. investigated the effective connections between different network modules and proposed a

hierarchical dense recursive network for image super-resolution [39]. Zhang et al. also considered the attention over the context, and developed a context reasoning attention network for image super-resolution [40]. Progressive exploration and generative adversarial network were also investigated by Yi et al. for super-resolution [41]. Zhang et al. also analyzed the image super-resolution in the fluid micelle perspective and proposed an FMNet for image super-resolution [42]. However, they do not concentrate on the mathematical analysis of the image super-resolution and only use end-to-end CNN to map the low-resolution (LR) images to high-resolution (HR) instances.

Recently researchers begin to investigate the interpretation of neural networks and design networks based on mathematical analysis. ADMM-Net [43] provides an optimization perspective analysis on compressive sensing MRI and designs an end-to-end network to simulate the alternating direction method of multipliers (ADMM) operation. IRCNN [20] proposes a general analysis of the image restoration issue and designs a denoiser prior to solve the problem based on the half-quadratic splitting (HQS) strategy. Ma et al. propose an ADMM-based unfolding network for image super-resolution [44]. Tuo et al. also consider real aperture super-resolution with an ADMM-based solver [45]. ISRN [22] is also investigated recently for single image super-resolution, which utilizes HQS to build an end-to-end iterative network. Zhang et al. rethink the degradation model of image super-resolution and propose a plug-and-play super-resolution network for arbitrary downsampling situations [46]. However, these works only regard the iterative scheme as guidance to design the network pipeline, but neglect to concentrate on the block architecture.

3. Methodology

In this section, we use Landweber [23] iteration method to analyze the image SR issue and design an end-to-end network to restore the image. Given a low-resolution (LR) image $\mathbf{I}^{\mathrm{LR}} \in R^{H\times W\times C}$, the task of image super-resolution is to find a corresponding high-resolution (HR) image $\mathbf{I}^{\mathrm{HR}} \in R^{sH\times sW\times C}$, satisfying

$$\mathbf{I}^{\mathrm{LR}} = \mathscr{D}\mathbf{I}^{\mathrm{HR}}, \tag{1}$$

where $\mathscr{D}$ is the degradation operation, H, $\mathbf{W}$, C are the height, width, and channels of the image separately, and s is the scaling factor. Usually $\mathscr{D}$ can be represented as a matrix. If D is a nonsingular matrix, then there is the specific solution for $\mathbf{I}^{\mathrm{HR}}$ where

$$\mathbf{I}^{HR} = \mathscr{D}^{-1}\mathbf{I}^{LR}. \tag{2}$$

However, due to the highly ill-conditioned property of the image SR problem, the solution of (1) is sensitive to the noise. Especially, if $\mathscr{D}$ is a singular matrix, there is no exact solution of $\mathbf{I}^{HR}$. As such, we try to find a least-squares super-resolution solution $\mathbf{I}^{SR}$ that satisfies

$$\mathbf{I}^{\mathrm{SR}} = \mathrm{argmin}_{\mathbf{I}^{\mathrm{SR}}}\frac{1}{2}\left\|\mathscr{D}\mathbf{I}^{\mathrm{SR}} - \mathbf{I}^{\mathrm{LR}}\right\|^2. \tag{3}$$

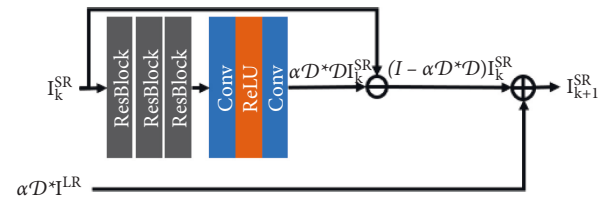

Figure 2: Block design of Landweber iteration step (LandBlock).

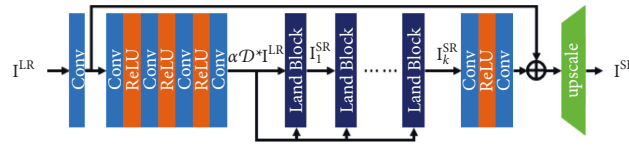

Figure 3: Network design. (a) $k = 0$. (b) $k = 4$. (c) $k = 8$. (d) $k = 12$. (e) $k = 16$.

To solve the issue, we consider the fix-point equation as

$$\mathbf{I}^{\mathrm{SR}} = \mathbf{I}^{\mathrm{SR}} + \mathscr{D}^*\left(\mathbf{I}^{\mathrm{LR}} - \mathscr{D}\mathbf{I}^{\mathrm{SR}}\right), \tag{4}$$

where $\mathscr{D}^*$ is the conjugate matrix of $\mathscr{D}$. The fix-point equation is converged at the point where $\mathbf{I}^{\mathrm{LR}} = \mathscr{D}\mathbf{I}^{\mathrm{SR}}$

As such, we use the iterative method to gradually update the $\mathbf{I}^{\mathrm{SR}}$ and find a feasible solution as

$$\mathbf{I}_{k+1}^{\mathrm{SR}} = \mathbf{I}_k^{\mathrm{SR}} + \mathscr{D}^*\left(\mathbf{I}^{\mathrm{LR}} - \mathscr{D}\mathbf{I}_k^{\mathrm{SR}}\right), \tag{5}$$

where $\mathbf{I}_k^{\mathrm{SR}}$ is the result of k-th iteration.

The (5) can be re-written as

$$\mathbf{I}_{k+1}^{\mathrm{SR}} = \left(I - \alpha\mathscr{D}^*\mathscr{D}\right)\mathbf{I}_k^{\mathrm{SR}} + \alpha\mathscr{D}^*\mathbf{I}^{\mathrm{LR}}. \tag{6}$$

which can be regarded as a gradient descent step. With the accumulate of iteration step k, the accuracy becomes higher.

The iteration mechanism inspires us to design a network and solve the problem, which learns the matrix representation from the training data pairs. Our block is designed based on the (6). Figure 2 shows the block design for Landweber iteration step. Three residual blocks [16], two convolutional layers, and one ReLU activation are designed to calculate the $\alpha\mathscr{D}^*\mathscr{D}\mathbf{I}_k^{\mathrm{SR}}$. The residual block follows the same design with EDSR [15], which is composed of two convolutional layers, one ReLU activation, and a skip connection. After calculation, the inputs is subtracted by the $\mathbf{I}_k^{\mathrm{SR}}$, and then added by the $\alpha\mathscr{D}^*\mathbf{I}^{\mathrm{LR}}$.

Figure 3 shows the entire network design. First, one convolutional layer processes the input $\mathbf{I}^{\mathrm{LR}}$ and gets the extracted feature map $\mathbf{x}^{\mathrm{LR}}$, which is described as

$$\mathbf{x}^{\mathrm{LR}} = \mathrm{Conv}\left(\mathbf{I}^{\mathrm{LR}}\right). \tag{7}$$

Then, four convolutional layers and three ReLU activation layers are utilized to calculate the $\alpha\mathscr{D}^*\mathbf{I}^{\mathrm{LR}}$ from the extracted feature map as

$$\alpha\mathscr{D}^*\mathbf{I}^{\mathrm{LR}} = \mathrm{extractor}\left(\mathbf{x}^{\mathrm{LR}}\right), \tag{8}$$

where $\mathrm{extractor}(\cdot)$ denotes the CNN layers.

There are Landweber iteration blocks (LandBlock) in the network to perform the optimization according to the (6). For the ith iteration, there is

$$\mathbf{I}_{i+1}^{\mathrm{SR}} = \mathrm{LandBlock}_i\left(\mathbf{I}_i^{\mathrm{SR}}, \alpha\mathscr{D}^*\mathbf{I}^{\mathrm{LR}}\right), \tag{9}$$

where $\mathrm{LandBlock}_i(\cdot)$ denotes the ith Landweber iteration block.

After kth iteration, there is a padding structure composed of two convolutional layers and a ReLU activation to process the feature map. Then, a skip connection is designed to learn the residual information and improve the gradient transmission [16] as

$$\mathbf{x}^{\mathrm{SR}} = \mathbf{x}^{\mathrm{LR}} + \mathbf{I}_k^{\mathrm{SR}}. \tag{10}$$

Finally, there is an upscale module to restore the SR image from the feature map, which is described as

$$\mathbf{I}^{\mathrm{SR}} = \mathrm{Upscale}\left(\mathbf{x}^{\mathrm{SR}}\right), \tag{11}$$

where $\mathrm{Upscale}(\cdot)$ is the upscale module composed of one convolutional layer and a subpixel convolution [30].

The implementation detail of LandNet is as follows. The number of iteration blocks is set as $k = 16$. All convolutional layers are with channel number as $c = 64$ except for the upscale module. The loss function is chosen as ℓ_1-norm.

4. Experiment

We train the network with DIV2K [47] data set. DIV2K data set contains 800 images for training and 100 images for validation. The images of DIV2K data set are with near 2K resolution, which are widely used in recent image SR works [7, 15, 17, 22]. We update our network for 1000 epoch by Adam optimizer [48] with learning rate $lr = 10^{-4}$. The patch size of training data is set as 48×48 for LR input. All other settings are same with RDN [17]. The testing benchmark is chosen as Set5 [49], Set14 [50], B100 [51], Urban100 [52], and Manga109 [53].

4.1. Ablation Study

4.1.1. Investigation on the Computational Complexity. To show the effectiveness of our LandNet, we compare the performance, the computational complexity, and the parameters with recent works: OISR [54], MSRN [55], MemNet [56], EDSR [15], and DBPN [57]. The computational complexity is modeled as the number of multiply-accumulate operations (MACs). The MACs is calculated by restoring a 720P image (1280×720) with the given scaling factor. Table 1 shows the MACs, parameters, and PSNR comparisons with scaling factor ×4. In the table, we can find our network achieves better performance than OISR and MSRN with fewer parameters and MACs. When compared with EDSR and DBPN, LandNet achieves competitive performance with much fewer parameters and MACs. Specially, LandNet holds near 10% parameters and MACs than EDSR and only drops 0.08 dB PSNR on Set5. Similarly, LandNet holds near 47% parameters and 5% MACs than DBPN while only suffers near 0.07 dB PSNR decrease. In this point of view, LandNet is proved to be an effective design for image super-resolution. Furthermore, we mainly compare our method with state-of-the-art methods (NLSN [38], CRAN [40]). In the table, we can find that NLSN has near 10 times MACs and parameters than LandNet with only 0.1 dB PSNR improvement on Set14. Similarly, CRAN has near 3 times MACs and parameters than LandNet, but only gains 0.3 dB PSNR improvement on Set5 and Set14. In this point of view, LandNet is an effective method for image super-resolution with restricted parameters and complexity.

Table 1: Computational complexity, parameters, and PSNR comparisons among different methods with scaling factor ×4.

Method	MACs (G) ↓	Params (M) ↓	Set 5 ↑	Set 14 ↑
OISR [54]	412.2	5.50	32.32	28.72
MSRN [55]	368.6	6.37	32.26	28.63
MemNet [56]	2662.4	0.67	31.74	28.26
EDSR [15]	2895.8	43.08	32.46	28.80
DBPN [57]	5213.0	10.42	32.47	28.81
NLSN [38]	2597.2	44.15	32.59	28.87
CRAN [40]	920.1	15.78	32.72	29.01
LandNet	286.2	4.97	32.39	28.74

4.1.2. Investigation on the Iterative Mechanism. To further investigate the effectiveness of iterative blocks, we demonstrate the results from different iterations. Figure 4 shows the output with different iteration blocks. In the figure, we can find that with the increase of iteration block k, the artifacts are more and more suppressed and the visual quality becomes better. This is in accordance with the mathematical analysis.

Furthermore, we also compare the objective performances of different iteration blocks. For a fair comparison, we train the different network under the same protocol for 200 epochs. Table 2 shows the average PSNR/SSIM results of different iterations. We can find that with the increase of the number of the iteration block k, the PSNR/SSIM results gradually increase. This is in accordance with the Landweber iteration that more iteration steps lead to more accurate solution.

4.1.3. Investigation on the Block Design. In the paper, we specially design the LandBlock to perform the iteration steps. To show the effectiveness of the block design, we compare our network with the modified version that substitutes the LandBlock with classical residual blocks. For a fair comparison, we train the different network under the same protocol for 200 epochs. Table 3 shows the PSNR/SSIM comparison. We can find that the LandBlock brings a significant improvement on all testing benchmarks, which demonstrate that the LandNet is an effective design.

4.2. Comparison with State-of-the-Art Methods. To show the performance of our LandNet, we compare our network with several traditional and recent works: SRCNN [13], FSRCNN [29], VDSR [14], DRCN [58], LapSRN [59], SelNet [60],

(a) $k = 0$ (b) $k = 4$ (c) $k = 8$ (d) $k = 12$ (e) $k = 16$

Figure 4: Results from different iterations. The output is generated from features of the k-th iteration block (a) $k = 0$ (b) $k = 4$ (c) $k = 8$ (d) $k = 12$ (e) $k = 16$.

Table 2: Average PSNR/SSIM results of different iteration blocks with degradation model BI ×4.

k	Set 5	Set 14	B 100	Urban 100
4	28.97/0.8275	26.69/0.7430	26.28/0.7103	24.46/0.7360
8	31.18/0.8706	28.07/0.7686	27.25/0.7291	25.47/0.7622
12	31.76/0.8822	28.40/0.7749	27.46/0.7324	25.84/0.7741
16	32.12/0.8943	28.59/0.7824	27.58/0.7363	26.16/0.7892

Table 3: Average PSNR/SSIM results of different blocks designs with degradation model BI ×4.

Block	Set5	Set14	B100
ResBlock	23.07/0.5112	22.26/0.4875	23.19/0.5303
Land	32.12/0.8943	28.59/0.7824	27.58/0.7363

RAN [61], DNCL [62], FilterNet [63], MRFN [64], SeaNet [65], DEGREE [66], FSN [67], MFSR [68], DSRLN [69], and MemNet [56]. The indicators are chosen as peak signal-to-noise ratio (PSNR) and structural similarity (SSIM). Table 4 shows the average PSNR/SSIM under degradation model bicubic-down (BI) with scaling factor ×2, ×3, and ×4 on five benchmarks. The best performances are shown in bold. The dash line means the paper does not report their performance.

In the table, we can find the proposed LandNet achieves the best performances on all five testing benchmarks and three scaling factors. When the scaling factor is ×2, LandNet achieves 0.4 and 0.3 PSNR improvements than the MFSR on Urban100 and Manga109 benchmarks separately. Similarly, when the scaling factors are ×3 and ×4, our network also achieves significant improvements on Urban100 and Manga109. It should be noticed that Urban100 is a data set with plentiful buildings, and Manga109 is a data set with comics, which contain a large amount of structural information. In this point of view, LandNet can effectively recover the high-frequency edge and structural information than other works.

Figure 5 shows the visual comparisons on Urban100 data set. We mainly compare our model with two representative methods: LapSRN [59] and Cross-SRN [7]. LapSRN is inspired by the Laplacian pyramid, which utilizes multiscale architecture to restore the structural information. Cross-SRN is specially designed to concentrate on the edges and lines. In the figure, we can find that LandNet achieves the best PSNR performance than other works. There is near 0.8 dB improvement on the two testing instances. In this point of view, the LandNet has superior structural information recovery capacity to other works. In the visual comparison, LandNet can recover more accurate lines. The results from LandNet are closest to the groundtruth.

Furthermore, we statistically verify the effectiveness of our methods. We conduct the two sample T-Test among LR, VDSR, and LandNet in pair to show the superiority of our method. Table 5 shows the two-sample T-Test comparisons. In the table, 0 means the left method performs statistically the same as the upper method. −1 means the left method performs worse than the upper method, and 1 means the left method performs better than the upper method. In the table, we can find that LandNet statistically improves the image quality and performs better than VDSR.

5. Discussion

5.1. Discussion on the Landweber Iteration. Landweber iteration is an effective method to solve the highly ill-conditioned problem such as image reconstruction [70–72]. It has been proved with strong convergence and the precision becomes higher with the increase of iteration steps [73]. The image reconstruction can be generally described as (1), by substituting the degradation $\mathscr{D}$ with different operations. There are numerous optimization methods to utilize the Landweber iteration method for image restoration [71, 74]. However, they highly rely on the explicit representation of the degradation $\mathscr{D}$, which is challenging for the image super-resolution task. As such, we propose a Landweber iteration-inspired network to adaptively learn the degradation representation and the solution from LR-HR pairs.

Table 4: Average PSNR/SSIM with degradation model BI ×2, ×3, and ×4 on five benchmarks. The best performances are shown in bold. The dash line means the paper does not report their performance.

Scale	Model	Set5 [50] PSNR/SSIM	Set14 [51] PSNR/SSIM	B100 [52] PSNR/SSIM	Urban100 [53] PSNR/SSIM	Manga109 [54] PSNR/SSIM
×2	SRCNN [13]	36.66/0.9542	32.42/0.9063	31.36/0.8879	29.50/0.8946	35.74/0.9661
	FSRCNN [29]	37.00/0.9558	32.63/0.9088	31.53/0.8920	29.88/0.9020	36.67/0.9694
	VDSR [14]	37.53/0.9587	33.03/0.9124	31.90/0.8960	30.76/0.9140	37.22/0.9729
	DRCN [58]	37.63/0.9588	33.04/0.9118	31.85/0.8942	30.75/0.9133	37.63/0.9723
	LapSRN [59]	37.52/0.9590	33.08/0.9130	31.80/0.8950	30.41/0.9100	37.27/0.9740
	SelNet [60]	37.89/0.9598	33.61/0.9160	32.08/0.8984	–	–
	RAN [61]	37.58/0.9592	33.10/0.9133	31.92/0.8963	–	–
	DNCL [62]	37.65/0.9599	33.18/0.9141	31.97/0.8971	30.89/0.9158	–
	FilterNet [63]	37.86/0.9610	33.34/0.9150	32.09/0.8990	31.24/0.9200	–
	MRFN [64]	37.98/0.9611	33.41/0.9159	32.14/0.8997	31.45/0.9221	38.29/0.9759
	SeaNet-baseline [65]	37.99/0.9607	33.60/0.9174	32.18/0.8995	32.08/0.9276	38.48/0.9768
	DEGREE [66]	37.58/0.9587	33.06/0.9123	31.80/0.8974	–	–
	FSN [67]	37.68/0.9065	33.51/0.9180	32.09/**0.9015**	31.68/0.9248	–
	MFSR [68]	38.07/0.9608	33.69/0.9191	32.22/0.9002	32.35/0.9307	38.75/0.9768
	LandNet (ours)	**38.13/0.9609**	**33.89/0.9203**	**32.31**/0.9013	**32.74/0.9340**	**39.05/0.9778**
×3	SRCNN [13]	32.75/0.9090	29.28/0.8209	28.41/0.7863	26.24/0.7989	30.59/0.9107
	FSRCNN [29]	33.16/0.9140	29.43/0.8242	28.53/0.7910	26.43/0.8080	30.98/0.9212
	VDSR [14]	33.66/0.9213	29.77/0.8314	28.82/0.7976	27.14/0.8279	32.01/0.9310
	DRCN [58]	33.82/0.9226	29.76/0.8311	28.80/0.7963	27.15/0.8276	32.31/0.9328
	DRRN [58]	34.03/0.9244	29.96/0.8349	28.95/0.8004	27.53/0.8378	32.74/0.9390
	SelNet [60]	34.27/0.9257	30.30/0.8399	28.97/0.8025	–	–
	RAN [61]	33.71/0.9223	29.84/0.8326	28.84/0.7981	–	–
	DNCL [62]	33.95/0.9232	29.93/0.8340	28.91/0.7995	27.27/0.8326	–
	FilterNet [63]	34.08/0.9250	30.03/0.8370	28.95/0.8030	27.55/0.8380	–
	MRFN [64]	34.21/0.9267	30.03/0.8363	28.99/0.8029	27.53/0.8389	32.82/0.9396
	SeaNet-baseline [65]	34.36/0.9280	30.34/0.8428	29.09/0.8053	28.17/0.8527	33.40/0.9444
	DEGREE [66]	33.76/0.9211	29.82/0.8326	28.74/0.7950	–	–
	DSRLN [69]	34.56/-	30.36/-	29.29/-	27.88/-	–
	MFSR [68]	34.49/0.9280	30.42/0.8442	29.16/0.8068	28.39/0.8577	33.72/0.9457
	LandNet (ours)	**34.60/0.9288**	**30.47/0.8453**	**29.20/0.8081**	**28.63/0.8626**	**33.91/0.9471**
×4	SRCNN [13]	30.48/0.8628	27.49/0.7503	26.90/0.7101	24.52/0.7221	27.66/0.8505
	FSRCNN [29]	30.71/0.8657	27.59/0.7535	26.98/0.7150	24.62/0.7280	27.90/0.8517
	VDSR [14]	31.35/0.8838	28.01/0.7674	27.29/0.7251	25.18/0.7524	28.83/0.8809
	DRCN [58]	31.53/0.8854	28.02/0.7670	27.23/0.7233	25.14/0.7510	28.98/0.8816
	LapSRN [59]	31.54/0.8850	28.19/0.7720	27.32/0.7280	25.21/0.7560	29.09/0.8845
	MemNet [56]	31.74/0.8893	28.26/0.7723	27.40/0.7281	25.50/0.7630	29.42/0.8942
	SelNet [60]	32.00/0.8931	28.49/0.7783	27.44/0.7325	–	–
	RAN [61]	31.43/0.8847	28.09/0.7691	27.31/0.7260	–	–
	DNCL [62]	31.66/0.8871	28.23/0.7717	27.39/0.7282	25.36/0.7606	–
	FilterNet [63]	31.74/0.8900	28.27/0.7730	27.39/0.7290	25.53/0.7680	–
	MRFN [64]	31.90/0.8916	28.31/0.7746	27.43/0.7309	25.46/0.7654	29.57/0.8962
	SeaNet-baseline [65]	32.18/0.8948	28.61/0.7822	27.57/0.7359	26.05/0.7896	30.44/0.9088
	DEGREE [66]	31.47/0.8837	28.10/0.7669	27.20/0.7216	–	–
	MFSR [68]	32.26/0.8961	28.65/0.7838	27.63/0.7381	26.25/0.7919	30.62/0.9103
	LandNet (ours)	**32.39/0.8975**	**28.74/0.7857**	**27.66/0.7395**	**26.46/0.7983**	**30.88/0.9134**

The values with bold type are the best ones within the experiments, which can show the advantages of our method in this paper.

Figure 4 shows the effectiveness of Landweber iteration. The images in the figure are results from different iterations. We can find that with the increase of iterations, the image becomes clearer and the quality is boosted. This is in accordance with the Landweber iteration that the result converges with the increase of iteration time k.

Different from straightforward end-to-end CNN methods for image reconstruction [13, 14, 29, 59], the Landweber iteration can find a more precise solution with the increase of iteration times. The optimization can adaptively adjust the descent direction with the help of the input. In this point of view, the Landweber iteration is more robust for finding a feasible solution, which is more suitable for solving the highly ill-conditioned image reconstruction issue. For the nonconvex optimization issue, Landweber iteration can find a good solution with higher PSNR/SSIM performance, as shown in Table 4.

5.2. Optimization Details. The parameter optimization is conducted by the Adam optimizer [48]. The Adam optimizer calculates the momentum for updating the network

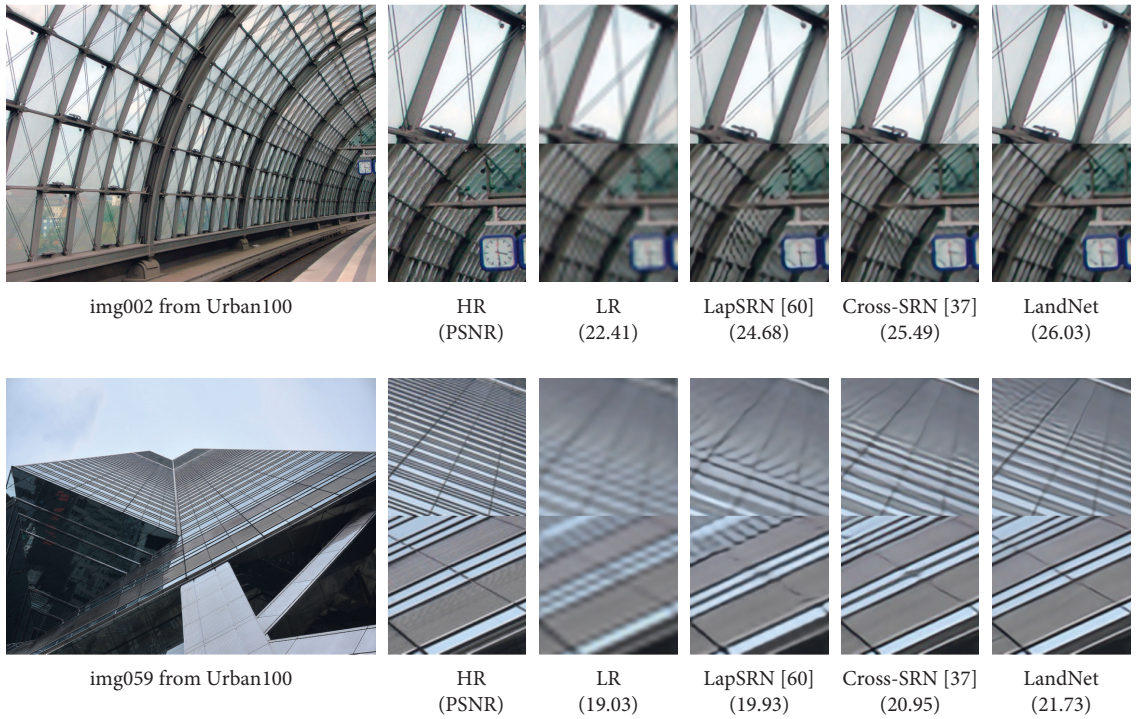

Figure 5: Visual comparisons on Urban100 benchmark.

Table 5: Two sample T-test comparisons among LR, VDSR, and our methods.

Method	LR	VDSR	LandNet
LR	0	−1	−1
VDSR	1	0	−1
LandNet	1	1	0

parameters. The learning rate is adaptively adjusted during the optimization step. We calculate the gradient of parameters by the back-propagation algorithm and use mean average error (MAE) to calculate the distance between the predict result and the label. We train our network for 1000 epochs. The batch size is set as 16, and the patch size is set as 48×48 for LR input.

6. Conclusion

In this paper, we proposed an end-to-end network for single image super-resolution. We investigated the image super-resolution problem in the optimization perspective and derived an iterative scheme to solve the problem based on the Landweber iteration. According to the mathematical analysis, we devised an convolutional neural network block to simulate the iterative step and perform the optimization. Based on the block, an end-to-end network is designed for image restoration, which is termed as LandNet. Experimental results show the proposed LandNet can achieve competitive or better subjective and objective performances than state-of-the-art methods with fewer parameters and computational cost.

Data Availability

All data, models, or code generated or used during the study are available from the corresponding author by request (lxb715@hotmail.com).

Conflicts of Interest

The authors declare no conflicts of interest in this paper.

Acknowledgments

This research was supported in part by the National Natural Science Foundation of China (No. 61802161) and the Department of Education of Liaoning Province (No. JZL202015402).

References

[1] R. Keys, "Cubic convolution interpolation for digital image processing," *IEEE Transactions on Acoustics, Speech, & Signal Processing*, vol. 29, no. 6, pp. 1153–1160, 1981.

[2] G. Tudavekar, S. R. Patil, and S. S. Saraf, "Dual-tree complex wavelet transform and super-resolution based video inpainting application to object removal and error concealment," *CAAI Transactions on Intelligence Technology*, vol. 5, no. 4, pp. 314–319, 2020.

[3] Q. Zou, K. Xiong, Q. Fang, and B. Jiang, "Deep imitation reinforcement learning for self-driving by vision," *CAAI Transactions on Intelligence Technology*, vol. 6, no. 4, pp. 493–503, 2021.

[4] X. Zhang and G. Wang, "Stud pose detection based on photometric stereo and lightweight yolov4," *Journal of Artificial Intelligence and Technology*, vol. 2, no. 1, pp. 32–37, 2022.

[5] L. Li, Z. Fan, M. Zhao et al., "Super-resolution reconstruction of underwater image based on image sequence generative adversarial network," *Mathematical Problems in Engineering*, vol. 2020, pp. 1–10, Article ID 8472875, 2020.

[6] Y. Liu, X. Zhang, S. Wang, S. Ma, and W. Gao, "Spatial-temporal correlation learning for real-time video deinterlacing," in *Proceedings of the IEEE International Conference on Multimedia and Expo (ICME)*, pp. 1–6, Shenzhen, China, July 2021.

[7] K. Nguyen, C. Fookes, S. Sridharan, and S. Denman, "Feature-domain super-resolution for iris recognition," *Computer Vision and Image Understanding*, vol. 117, no. 10, pp. 1526–1535, 2021.

[8] X. Zhang, K. Cao, and L. Jiao, "A contourlet-based interpolation restoration method for super-resolution of sar image," in *Proceedings of the Asian-Pacific Conference on Synthetic Aperture Radar*, pp. 1068–1071, Xi'an, China, October 2009.

[9] Liyakathunisa and C. R. Kumar, "A novel wavelet based super resolution reconstruction of low resolution images using adaptive interpolation," in *Proceedings of the International Conference on Advances in Recent Technologies in Communication and Computing*, pp. 146–150, Kottayam, India, October 2010.

[10] Y. Zhang, Q. Fan, F. Bao, Y. Liu, and C. Zhang, "Single-image super-resolution based on rational fractal interpolation," *IEEE Transactions on Image Processing*, vol. 27, no. 8, pp. 3782–3797, 2018.

[11] C. Shousen, J. Quanzhu, and X. Qiang, "Image super-resolution reconstruction based on compressed sensing," in *Proceedings of the International Conference on Information Science and Control Engineering (ICISCE)*, pp. 368–374, Changsha, China, July 2017.

[12] Y. Zhao, Y. Yang, Q. Zhang, J. Yang, and J. Li, "Hyperspectral imagery super-resolution by image fusion and compressed sensing," in *Proceedings of the IEEE International Geoscience and Remote Sensing Symposium*, pp. 7260–7262, Munich, Germany, July 2012.

[13] C. Dong, C. C. Loy, K. He, and X. Tang, "Image super-resolution using deep convolutional networks," *IEEE Transactions on Pattern Analysis and Machine Intelligence*, vol. 38, no. 2, pp. 295–307, 2016.

[14] J. Kim, J. K. Lee, and K. M. Lee, "Accurate image super-resolution using very deep convolutional networks," in *Proceedings of the IEEE Conference on Computer Vision and Pattern Recognition (CVPR)*, pp. 1646–1654, Las Vegas, NV, USA, June 2016.

[15] B. Lim, S. Son, H. Kim, S. Nah, and K. M. Lee, "Enhanced deep residual networks for single image super-resolution," in *Proceedings of the IEEE Conference on Computer Vision and Pattern Recognition Workshops (CVPRW)*, pp. 1132–1140, Honolulu, HI, USA, July 2017.

[16] K. He, X. Zhang, S. Ren, and J. Sun, "Deep residual learning for image recognition," in *Proceedings of the IEEE Conference on Computer Vision and Pattern Recognition (CVPR)*, pp. 770–778, Las Vegas, NV, USA, June 2016.

[17] Y. Zhang, Y. Tian, Y. Kong, B. Zhong, and Y. Fu, "Residual dense network for image restoration," *IEEE Transactions on Pattern Analysis and Machine Intelligence*, vol. 43, no. 7, pp. 2480–2495, 2021.

[18] Y. Guo, J. Chen, J. Wang et al., "Closed-loop matters: dual regression networks for single image super-resolution," in *Proceedings of the IEEE/CVF Conference on Computer Vision and Pattern Recognition (CVPR)*, pp. 5406–5415, Seattle, WA, USA, June 2020.

[19] J. Liu, W. Zhang, Y. Tang, J. Tang, and G. Wu, "Residual feature aggregation network for image super-resolution," in *Proceedings of the IEEE/CVF Conference on Computer Vision and Pattern Recognition*, pp. 2356–2365, Seattle, WA, USA, June 2020.

[20] K. Zhang, W. Zuo, S. Gu, and L. Zhang, "Learning deep CNN denoiser prior for image restoration," in *Proceedings of the IEEE Conference on Computer Vision and Pattern Recognition*, pp. 2808–2817, Honolulu, HI, USA, July 2017.

[21] S.-W. Hu, G.-X. Lin, and C.-S. Lu, "Gpx-admm-net: interpretable deep neural network for image compressive sensing," *IEEE Access*, vol. 9, Article ID 158695, 2021.

[22] Y. Liu, S. Wang, J. Zhang, S. Wang, S. Ma, and W. Gao, "Iterative network for image super-resolution," *IEEE Transactions on Multimedia*, vol. 24, no. 1–1, pp. 2259–2272, 2022.

[23] A. Neubauer, "On landweber iteration for nonlinear ill-posed problems in hilbert scales," *Numerische Mathematik*, vol. 85, no. 2, pp. 309–328, 2000.

[24] M. Sajid, N. Ali, N. I. Ratyal, S. H. Dar, and B. Zafar, "Facial asymmetry-based feature extraction for different applications: a review complemented by new advances," *Artificial Intelligence Review*, vol. 54, no. 6, pp. 4379–4419, 2021.

[25] N. Ali, K. B. Bajwa, R. Sablatnig, and Z. Mehmood, "Image retrieval by addition of spatial information based on histograms of triangular regions," *Computers & Electrical Engineering*, vol. 54, pp. 539–550, 2016.

[26] J. Li, K. Wattanachote, and Y. Wu, "Maximizing nonlocal self-similarity prior for single image super-resolution," *Mathematical Problems in Engineering*, vol. 2019, pp. 1–14, Article ID 3840285, 2019.

[27] L.-L. Huang, L. Xiao, and Z.-H. Wei, "Efficient and effective total variation image super-resolution: a preconditioned operator splitting approach," *Mathematical Problems in Engineering*, vol. 2011, pp. 1–20, Article ID 380807, 2011.

[28] Z. Huang, W. Zheng, L. Yan, and C. Gou, "A novel face super-resolution method based on parallel imaging and openvino," *Mathematical Problems in Engineering*, vol. 2021, pp. 1–9, Article ID 6648983, 2021.

[29] C. Dong, C. C. Loy, and X. Tang, "Accelerating the super-resolution convolutional neural network," in *Computer Vision - ECCV 2016*, B. Leibe, J. Matas, N. Sebe, and M. Welling, Eds., vol. 9906, pp. 391–407, Springer, NY, USA, 2016.

[30] W. Shi, J. Caballero, F. Huszar et al., "Real-time single image and video super-resolution using an efficient sub-pixel convolutional neural network," in *Proceedings of the IEEE Conference on Computer Vision and Pattern Recognition*, pp. 1874–1883, IEEE Computer Society, Las Vegas, NV, USA, June 2016.

[31] T. Tong, G. Li, X. Liu, and Q. Gao, "Image super-resolution using dense skip connections," in *Proceedings of the IEEE International Conference on Computer Vision*, pp. 4809–4817, IEEE Computer Society, Venice, Italy, October 2017.

[32] G. Huang, Z. Liu, L. van der Maaten, and K. Q. Weinberger, "Densely connected convolutional networks," in *Proceedings of the IEEE Conference on Computer Vision and Pattern Recognition*, pp. 2261–2269, Honolulu, HI, USA, July 2017.

[33] Y. Zhang, K. Li, K. Li, L. Wang, B. Zhong, and Y. Fu, "Image super-resolution using very deep residual channel attention networks," *Computer Vision - ECCV 2018*, vol. 11211, pp. 294–310, 2018.

[34] J. Hu, L. Shen, and G. Sun, "Squeeze-and-excitation networks," in *Proceedings of the IEEE Conference on Computer*

Vision and Pattern Recognition, pp. 7132–7141, Salt Lake City, UT, USA, June 2018.

[35] T. Dai, J. Cai, Y. Zhang, S. Xia, and L. Zhang, "Second-order attention network for single image super-resolution," in *Proceedings of the IEEE Conference on Computer Vision and Pattern Recognition*, Article ID 11065, Long Beach, CA, USA, June 2019.

[36] J. Liu, J. Tang, and G. Wu, "Residual feature distillation network for lightweight image super-resolution," in *Computer Vision - ECCV 2020 Workshops*vol. 12537, , pp. 41–55, Springer, 2020.

[37] X. Zhu, L. Zhang, L. Zhang, X. Liu, Y. Shen, and S. Zhao, "Gan-based image super-resolution with a novel quality loss," *Mathematical Problems in Engineering*, vol. 2020, pp. 1–12, Article ID 5217429, 2020.

[38] Y. Mei, Y. Fan, and Y. Zhou, "Image super-resolution with non-local sparse attention," in *Proceedings of the 2021 IEEE/CVF Conference on Computer Vision and Pattern Recognition (CVPR)*, pp. 3516–3525, 2021.

[39] K. Jiang, Z. Wang, P. Yi, and J. Jiang, "Hierarchical dense recursive network for image super-resolution," *Pattern Recognition*, vol. 107, Article ID 107475, 2020.

[40] Y. Zhang, D. Wei, C. Qin, H. Wang, H. Pfister, and Y. Fu, "Context Reasoning Attention Network for Image Super-resolution," in *Proceedings of the 2021 IEEE/CVF International Conference on Computer Vision (ICCV)*, pp. 4258–4267, 2021.

[41] P. Yi, Z. Wang, K. Jiang, J. Jiang, T. Lu, and J. Ma, "A progressive fusion generative adversarial network for realistic and consistent video super-resolution," *IEEE Transactions on Pattern Analysis and Machine Intelligence*, vol. 44, no. 5, 2021.

[42] M. Zhang, Q. Wu, J. Zhang, X. Gao, J. Guo, and D. Tao, "Fluid micelle network for image super-resolution reconstruction," *IEEE Transactions on Cybernetics*, no. 1–14, pp. 1–14, 2022.

[43] Y. Yang, J. Sun, H. Li, and Z. Xu, "Deep admm-net for compressive sensing MRI," in *Proceedings of the 30th Conference on Neural Information Processing Systems*, pp. 10–18, Barcelona, Spain, December 2016.

[44] Q. Ma, J. Jiang, X. Liu, and J. Ma, "Deep unfolding network for spatiospectral image super-resolution," *IEEE Transactions on Computational Imaging*, vol. 8, pp. 28–40, 2022.

[45] X. Tuo, Y. Xia, Y. Zhang et al., "Super-resolution imaging for real aperture radar by two-dimensional deconvolution," in *Proceedings of the IEEE International Geoscience and Remote Sensing Symposium IGARSS*, pp. 6630–6633, Brussels, Belgium, July 2021.

[46] K. Zhang, W. Zuo, and L. Zhang, "Deep plug-and-play super-resolution for arbitrary blur kernels," in *Proceedings of the IEEE Conference on Computer Vision and Pattern Recognition*, pp. 1671–1681, Long Beach, CA, USA, June 2019.

[47] E. Agustsson and R. Timofte, "Ntire 2017 challenge on single image super-resolution: dataset and study," in *Proceedings of the IEEE Conference on Computer Vision and Pattern Recognition Workshops*, pp. 1122–1131, Honolulu, HI, USA, July 2017.

[48] D. P. Kingma and J. Ba, "Adam: a method for stochastic optimization," in *Proceedings of the International Conference on Learning Representations*, 2015.

[49] M. Bevilacqua, A. Roumy, C. Guillemot, and M.-l. A. Morel, "Low-complexity single-image super-resolution based on nonnegative neighbor embedding," *Procedings of the British Machine Vision Conference 2012*, vol. 10, p. 135, 2012.

[50] R. Zeyde, M. Elad, and M. Protter, "On single image scale-up using sparse-representations," in *Curves and Surfaces*, pp. 711–730, Springer Berlin Heidelberg, Berlin, Heidelberg, 2012.

[51] D. Martin, C. Fowlkes, D. Tal, and J. Malik, "A database of human segmented natural images and its application to evaluating segmentation algorithms and measuring ecological statistics," in *Proceedings of the IEEE International Conference on Computer Vision*, vol. 2, pp. 416–423, Vancouver, BC, Canada, July 2001.

[52] J. Huang, A. Singh, and N. Ahuja, "Single image super-resolution from transformed self-exemplars," in *Proceedings of the IEEE Conference on Computer Vision and Pattern Recognition*, pp. 5197–5206, Boston, MA, USA, June 2015.

[53] Y. Matsui, K. Ito, Y. Aramaki et al., "Sketch-based manga retrieval using manga109 dataset," *Multimedia Tools and Applications*, vol. 76, no. 20, Article ID 21811, 2017.

[54] X. He, Z. Mo, P. Wang, Y. Liu, M. Yang, and J. Cheng, "Ode-inspired network design for single image super-resolution," in *Proceedings of the IEEE Conference on Computer Vision and Pattern Recognition (CVPR)*, pp. 1732–1741, Long Beach, CA, USA, June 2019.

[55] J. Li, F. Fang, K. Mei, and G. Zhang, "Multi-scale residual network for image super-resolution," in *Proceedings of the European Conference on Computer Vision (ECCV)*, vol. 2108, pp. 517–532, 2018.

[56] Y. Tai, J. Yang, X. Liu, and C. Xu, "Memnet: a persistent memory network for image restoration," in *Proceedings of the IEEE International Conference on Computer Vision*, pp. 4549–4557, Venice, Italy, October 2017.

[57] M. Haris, G. Shakhnarovich, and N. Ukita, "Deep back-projection networks for single image super-resolution," in *IEEE Transactions on Pattern Analysis and Machine Intelligence*, vol. 43, no. 12, pp. 4323–4337, 2020.

[58] J. Kim, J. K. Lee, and K. M. Lee, "Deeply-recursive convolutional network for image super-resolution," in *Proceedings of the IEEE Conference on Computer Vision and Pattern Recognition (CVPR)*, pp. 1637–1645, Las Vegas, NV, USA, June 2016.

[59] W.-S. Lai, J.-B. Huang, N. Ahuja, and M.-H. Yang, "Fast and accurate image super-resolution with deep laplacian pyramid networks," *IEEE Transactions on Pattern Analysis and Machine Intelligence*, vol. 41, no. 11, pp. 2599–2613, 2019.

[60] J. Choi and M. Kim, "A deep convolutional neural network with selection units for super-resolution," in *Proceedings of the IEEE Conference on Computer Vision and Pattern Recognition Workshops*, pp. 1150–1156, Honolulu, HI, USA, July 2017.

[61] Y. Wang, L. Wang, H. Wang, and P. Li, "Resolution-aware network for image super-resolution," *IEEE Transactions on Circuits and Systems for Video Technology*, vol. 29, no. 5, pp. 1259–1269, 2019.

[62] C. Xie, W. Zeng, and X. Lu, "Fast single-image super-resolution via deep network with component learning," *IEEE Transactions on Circuits and Systems for Video Technology*, vol. 29, no. 12, pp. 3473–3486, 2019.

[63] F. Li, H. Bai, and Y. Zhao, "Filternet: adaptive information filtering network for accurate and fast image super-resolution," *IEEE Transactions on Circuits and Systems for Video Technology*, vol. 30, no. 6, pp. 1511–1523, 2020.

[64] Z. He, Y. Cao, L. Du et al., "MRFN: multi-receptive-field network for fast and accurate single image super-resolution," *IEEE Transactions on Multimedia*, vol. 22, no. 4, pp. 1042–1054, 2020.

[65] F. Fang, J. Li, and T. Zeng, "Soft-edge assisted network for single image super-resolution," *IEEE Transactions on Image Processing*, vol. 29, pp. 4656–4668, 2020.

[66] W. Yang, J. Feng, J. Yang et al., "Deep edge guided recurrent residual learning for image super-resolution," *IEEE Transactions on Image Processing*, vol. 26, no. 12, pp. 5895–5907, 2017.

[67] S. Li, Q. Cai, H. Li, J. Cao, L. Wang, and Z. Li, "Frequency separation network for image super-resolution," *IEEE Access*, vol. 8, pp. 33768–33777, 2020.

[68] X. Liu, L. Wang, X. Chen, and Y. Liu, "Multilevel feature exploration network for image superresolution," *Scientific Programming*, vol. 2022, pp. 1–9, Article ID 2014627, 2022.

[69] T. Geng, X.-Y. Liu, X. Wang, and G. Sun, "Deep shearlet residual learning network for single image super-resolution," *IEEE Transactions on Image Processing*, vol. 30, pp. 4129–4142, 2021.

[70] B. Sullivan and H.-C. Chang, "A generalized landweber iteration for ill-conditioned signal restoration," *[Proceedings] ICASSP 91: 1991 International Conference on Acoustics, Speech, and Signal Processing*, vol. 3, pp. 1729–1732, 1991.

[71] P. Wang and H. Zhou, "Adaptive landweber image reconstruction with an optimal presetting method," in *Proceedings of the 2013 Ninth International Conference on Natural Computation (ICNC)*, pp. 1289–1293, Shenyang, China, July 2013.

[72] S. Gao and G. Qu, "Filter-based landweber iterative method for reconstructing the light field," *IEEE Access*, vol. 8, Article ID 138340, 2020.

[73] H. Trussell and M. Civanlar, "The landweber iteration and projection onto convex sets," *IEEE Transactions on Acoustics, Speech, & Signal Processing*, vol. 33, no. 6, pp. 1632–1634, 1985.

[74] X. Liu and C. Yan, "Application of improved landweber algorithm for ect image reconstruction," in *Proceedings of the 2021 17th International Conference on Computational Intelligence and Security (CIS)*, pp. 294–298, Chengdu, China, November 2021.